



## Research paper

# Prediction of concrete life under coupled dry and wet-sulfate erosion based on damage evolution equation

Nan Nie<sup>1</sup>

**Abstract:** In a corrosive environment with coupled dry-wet-sulfate action, concrete structures are susceptible to erosion by sulfate ions, which seriously affects the safe operating life. To forecast the operational lifetime of concrete below the influence of the dry-wet cycle and sulfate erosion environment, four different admixtures of polypropylene fiber: 0, 0.6, 0.9, and 1.2 kg/m<sup>3</sup>, were incorporated into concrete specimens, and indoor accelerated tests were designed to observe the macroscopic and microscopic deterioration law analysis of concrete specimens; using the precept of damage mechanics, the damage of concrete under solubility cycle was established. The damage evolution equation of concrete under freeze-thaw cycles was established and the operational life of concrete was predicted. The results showed that the overall mass loss rate of concrete specimens increased with the number of tests, and the relative energetic modulo decreased with the number of tests; the pore change pattern, microstructure, and internal material composition of specimens under different working conditions were obtained by using NMR scanning technique, SEM electron microscope scanning technique and XRD physical phase analysis technique. The damage evolution equation shows that adding a certain amount of polypropylene fiber to concrete can improve the working life of concrete under dry and wet connected sulfate assault.

**Keywords:** dry and wet-sulfate attack, concrete, polypropylene fiber, accelerated indoor testing, damage mechanics, life prediction

<sup>1</sup>MSc., Eng., Senior Engineer, Station Building Construction Department, China Railway Guangzhou Bureau Group Co., China, e-mail: [93604377@qq.com](mailto:93604377@qq.com) ORCID: 0000-0003-0374-3478

## 1. Introduction

With the continuous development of construction technology, due to the influence of factors such as internal changes in concrete materials or service environment, many concrete structures deteriorate in advance and their operating life is greatly shortened, and structural safety cannot be guaranteed, which threatens people's lives and property safety. Therefore, how to accurately predict concrete's operating life, improve concrete's durability, and achieve the sustainable development of construction projects has become the focus of current research.

The cause of concrete damage is, on the one hand, sulfate into the concrete, due to changes in the environment and other factors, sulfate crystallization precipitation, and the internal concrete due to expansion stress damage; on the other hand, sulfate and hydration products reaction, the resulting expansive products make the internal produce more cracks and make the cracks expand, which is conducive to the further transmission of sulfate, accelerating the process of concrete deterioration. Due to the special geographical conditions, large structures such as bridges, stations, and water conservancies in South China not only suffer from seasonal wet and dry cycle damage, but also from sulfate erosion damage in groundwater or lakes, which is more obvious and more serious deterioration than single factors. L.K. Ning et al. [1] used iron ore tailings (IOTs) as ecological composites instead of river sand to conduct iron ore tailings concrete (IOTC) performance tests and obtained that IOTC with 40% IOTs had the minimum porosity and denser microlevel, which significantly improved the denseness of IOTC. S. Alan, et al. [2] evaluated the performance of green concrete with mixed cement with different scrap glass powder content for long-term sulfate resistance, it was concluded that concrete with 50% glass aggregate was comparable to the sulfate resistance produced by natural aggregates in terms of sulfate resistance. T.W. Zewdu, et al. [3] used machine learning algorithms to predict the endurance and operating life of strengthened concrete buildings in coastal areas or chlorine-containing environments. The validation results confirmed that the support vector machine algorithm performed the best. C.H.X. Chen. [4] formulated concrete with some recycled aggregates in natural aggregates and conducts experimental research on the strength dispersion of concrete. M.C. Chen, et al. [5] based on the injure evolution model, the fatigue life of the test beam was predicted under the combined action of the scattered current, chloride ions, and fatigue loading. E. Zgheib, et al. [6] study of the effects of admixtures added to concrete using Bayesian linear regression methods. B. Vakhshouri, et al. [7] used compressive strength, modulus of elasticity and split tensile strength as indicators, and validated the ANFIS analytical model by multifactor linear regression analysis.

In recent years, researchers under the single-factor and coupled effects of defrost cycles and sulfate erosion have conducted a lot of research on concrete's durability at home and abroad, and have made certain achievements in the study of concrete life prediction, but there are still some problems, mainly including.

1. Although previous studies have analyzed the effects of different water-cement ratios, mineral admixtures and different admixtures on the execution of concrete enslaved to freeze-thaw or sulfate assault, the objects of the studies are concrete under standard curing conditions, and the early-age concrete is less involved.

2. Previous studies have established a large number of erosion damage models for concrete durability, but most of them are purely mathematical and statistical models based on experimental results, which are diverse but not widely applicable, and the perfection of the models needs further improvement.

This study takes the Guangzhou Baiyun station project as the background, combines the actual climatic environment of the project, designs and carries out a series of tests on the endurance of concrete under the connection effect of dry and wet cycles and sulfate erosion, analyzes the deterioration law of its performance under different working conditions, carries out the durability test of early-age concrete under the coupling effect of dry and wet cycles and sulfate erosion, explores the change law of concrete appearance, quality, compressive strength, and energetic flexible modulo. Based on the damage machinist theory, the concrete damage evolution model under different test regimes is proposed to further predict the operating life of the concrete.

## 2. Experimental overview

### 2.1. Test material

The test raw materials include water (tap water in the region with good water quality), P.O 42.5 common silicate cement, fine aggregate (natural river sand with 2.75 precision modulo), Coarse aggregate (5–15 mm particle size), polypropylene fiber (using the binding effect of the fiber to reduce the degree of cracking inside the concrete and to compare with ordinary concrete) and sulfate (to simulate the actual project suffered from Sulfate attack, anhydrous sodium sulfate ( $\text{Na}_2\text{SO}_4$ ) was used for sulfate attack test). The physical properties of the polypropylene fibers used in the test are shown in Table 1, and the chemical parameters of the sulfate are shown in Table 2. The data in the Table 1 and Table 2 comes from raw material purchasers.

Table 1. Physical properties of polypropylene fibers

Color	Shape	Density ( $\text{g}\cdot\text{m}^{-3}$ )	Length (mm)	Diameter ( $\mu\text{m}$ )	Tensile strength (MPa)	Modulo of elasticity (MPa)	Elongation at break (%)
White	Bunched monofilament	0.91	19	31.2	565	5900	27

Table 2. Chemical parameters of anhydrous sodium sulfate

Content ( $\text{Na}_2\text{SO}_4$ ) (w/%)	PH value (50 g/L 25°C)	Sodium chloride (NaCl) (w/%)	Phosphate ( $\text{SO}_4$ ) (w/%)	Total Nitrogen (N) (w/%)	Potassium (K) (w/%)	Calcium (Ca) (w/%)	Iron (Fe) (w/%)
$\geq 99.0$	5.0–8.0	$\leq 0.001$	$\leq 0.001$	$\leq 0.0005$	$\leq 0.001$	$\leq 0.002$	$\leq 0.0005$

## 2.2. Concrete mix ratio design

In this paper, the water-cement ratio of concrete is 0.43 and the large-scale proportion of cement, fine aggregate, and coarse aggregate are 1:1.45:2.94. Polypropylene fiber concrete was prepared by the fiber exclusion method, and three different fiber admixtures of 0.6, 0.9, and 1.2 kg/m<sup>3</sup> were considered in the design, and the comparison test was conducted with the normal water-cement ratio concrete, and the specific parameters are shown in Table 3.

Table 3. Parameters of 19 mm polypropylene fiber specimen

Specimen name	Polypropylene fiber dosing (kg/m <sup>3</sup> )	Specimen name	Polypropylene fiber dosing (kg/m <sup>3</sup> )
Q1	0	Q3	0.9
Q2	0.6	Q4	1.2

## 2.3. Test program

To study the deterioration law of cement samples under the action of dry and wet cycle-sulfate erosion, the dry and wet cycle-sulfate corrosion test protocol developed concerning literature [8,9] and specifications is as follows, The specific test procedure is shown in Fig. 1.

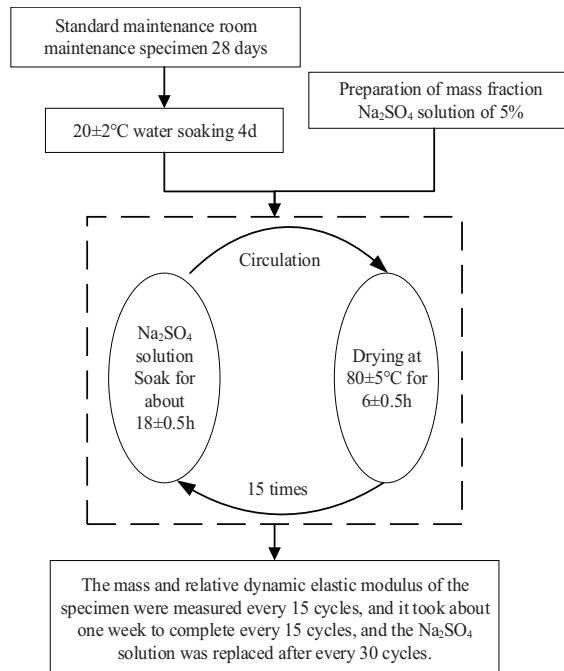


Fig. 1. Wet and dry – sulfate erosion flow chart

1. The specimens are taken out from the calibration room 2 days in advance (28 dage), dried on the surface of the specimens, and placed in an oven at  $80 \pm 5^\circ\text{C}$  for 48 hours and then cooled to room temperature.
2. Place the specimens in the specimen box, keeping a spacing of 50 mm between specimens, and the spacing between the specimens and the side walls of the specimen box is not less than 20 mm.
3. Pour a 5% mass fraction solution of  $\text{Na}_2\text{SO}_4$  into the specimen box and soak it for  $18 \pm 0.5$  h.
4. The soaked exemplars were taken out and arranged in the oven for  $6 \pm 0.5$  h. This is a cycle, and the specimens' large-scale and energetic elastic modulo was measured 15 times per cycle.

### 3. Experimental results and analysis

#### 3.1. Quality loss

The trend of the large-scale loss rate of each group of exemplars with the number of cycles is shown in Fig. 2.

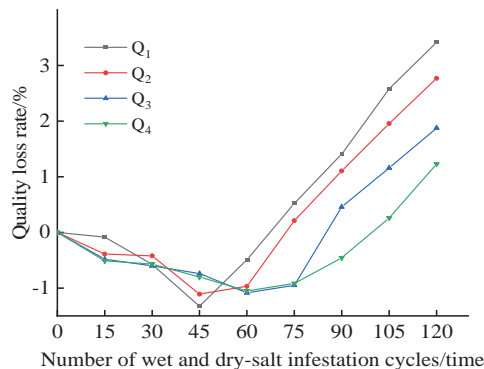


Fig. 2. Change curve of mass loss rate of specimens under the action of wet and dry-salt attack

The figure shows that the large-scale loss rate of each group of exemplars decreased and then increased as the test proceeded, in which the large-scale loss rate of exemplars in the Q1 and Q2 groups decreased to  $-1.33\%$  and  $-1.11\%$  after 45 dry-wet-sulfate erosions, and then the large-scale loss rate of exemplars in Q1 group began to increase linearly until the end of the test, and the difference with Q1 group is that the increase process of specimens in Q2 group had The inflection point of Q3 and Q4 growers were slightly lagged compared with Q1 and Q2 groups, and the mass loss rate of both groups reached the lowest point only after 60 dry and wet-sulfate erosion and the mass loss rates of both groups were  $-1.09\%$  and  $-1.05\%$  respectively when they reached the lowest point, after which the mass loss rates of both groups started to increase and the increase of Q3 group specimens was larger than that of Q4 group.

According to the trend of the mass loss rate of the specimen in Fig. 2, the specimen under the action of dry and wet cycle-sulfate erosion will first appear the phenomenon of slow weight gain, that is, the mass of the specimen is larger than its initial mass. This is because the specimens shed less in the early stage of the test and the solution contains a large amount of  $\text{SO}_2^{2-}$ , these  $\text{SO}_2^{2-}$  enter the specimen with the pore water to form new AFt, this newly formed AFt firstly occupy the pore space inside the specimen and remain inside the specimen; and due to the effect of the wet and dry cycle, the concentration of  $\text{SO}_2^{2-}$  ions inside the specimen is further increased, these  $\text{SO}_2^{2-}$  ions are partially connected with the  $\text{Ca}^{2+}$ ,  $\text{Mg}^{2+}$ , etc. to form insoluble sulfate inside the specimen, thus causing the increase of specimen mass. In the later stage of the test, as the solution can provide enough  $\text{SO}_2^{2-}$  for the formation of AFt, the continuously generated AFt fills the pores inside the specimen and then starts to generate expansion stress to crack the pores of the specimen, which exposes a larger contact surface after the pores are cracked and generate more AFt to form a vicious circle, which eventually leads to the specimen starting to fall off, thus the phenomenon of increasing and then decreasing the mass in the above figure. Comparing the sequence of increasing to decreasing inflection points of Q1, Q2, Q3, and Q4, we can see that the binding effect of polypropylene fibers can slow down the cracking inside the specimen to a certain extent and retard the generation of AFt, but this binding effect is limited. When the expansion stress generated by AFt is too large, the binding effect of the fibers ceases to exist and the specimens start to fall off significantly.

### 3.2. Relative dynamic modulo of elasticity

The corresponding relative dynamic elastic modulo variation curves are shown in Fig. 3.

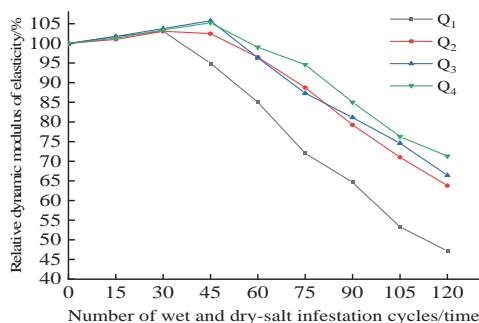


Fig. 3. Change curve of relative dynamic elastic modulo of specimens under dry and wet-sulfate erosion

It can be seen from the figure that with the dry and wet-sulfate erosion test, the energetic flexible modulo of the exemplars showed a tendency of first increasing and then decreasing, among which the inflection point of the energetic flexible modulo of the exemplars the common specimen Q1 appeared earlier than that of the polypropylene fiber specimens. The increase in the proportional energetic flexible modulo of the Q3 and Q4 specimens

was similar, at about 5%. There are two major reasons for the increase in the dynamic elastic moduli of the specimens: first, due to the high temperature of drying, the specimens contain a small amount of water in the internal pores, which produces a phenomenon similar to steam curing; second, the “wet” process during the wet and dry cycles of the test is carried out in the 5% mass fraction  $\text{Na}_2\text{SO}_4$  solution, so a large amount of  $\text{Na}_2\text{SO}_4$  through the pores of the specimen, and some of the free  $\text{SO}_4^{2-}$  ions react with the specimen to produce AFt, gypsum and other substances, and the “dry” process in the dry and wet cycle leads to the evaporation of water from the pores inside the specimen, which makes the concentration of  $\text{Na}_2\text{SO}_4$  solution increase to saturation and precipitate  $\text{Na}_2\text{SO}_4 \cdot 10\text{H}_2\text{O}$  crystals. These newly generated substances fill the native pores of the specimen and become the basic skeleton of the specimen, which improves the compactness and strength of the specimen. Subsequently, the relative dynamic elastic moduli of the specimen began to decline, mainly due to the intensification of the “two” reaction in the above reasons, and a large amount of  $\text{Na}_2\text{SO}_4$  solution entered the specimen to generate swelling AFt, gypsum, and  $\text{Na}_2\text{SO}_4 \cdot 10\text{H}_2\text{O}$ , etc, which eventually led to the internal cracking of the specimen and the decrease of strength, while the specimen with polypropylene fibers was filled with the new material. The specimens doped with polypropylene fibers, under the effect of fiber binding, played a role in retarding the internal cracking of the specimens to a certain extent, which in turn reduced the decrease in the dynamic elastic moduli of the specimens.

Early in the test, the inflection point of Q1 was earlier than the other three groups of specimens and the increase of relative dynamic elastic moduli of Q1 and Q2 was slightly smaller than that of Q3 and Q4, mainly because the incorporation of polypropylene fiber would increase the native pore space of the specimens, which led to the lower initial strength of the specimens. After the start of the test, due to more pores inside the polypropylene fiber specimens, the increase of strength under the action of “I” and “II” mentioned above is correspondingly larger, so the above phenomenon occurs. The earlier inflection point of Q1 further indicates that the specimens of Q1 reached the maximum strength earlier and were the first to start the strength decrease due to the absence of the binding effect of polypropylene fibers.

### 3.3. Nuclear magnetic resonance pore characterization

The variation of  $T_2$  spectral curves with the number of dry and wet-sulfate erosion for the two groups of specimens Q1, and Q3 obtained from NMR scans is shown in Fig. 4a and 4b.

From Fig. 4a and 4b, it can be seen that the locations of peaks 1 and 2 in the  $T_2$  spectral curves of the two groups of specimens were gradually shifted to the right with the number of dry and wet salt attack, in which the relaxation time of peak 1 in the Q1 group of specimens was shifted to the right from 0.9116 ms at the beginning to 1.8252 ms at the end of the test, and the relaxation time of peak 2 was shifted to the right from 27.3644 ms at the beginning to 357.0768 ms at the end of the test. The relaxation time of peak 1 of the Q3 group is the same as that of the Q1 group, and the relaxation time of peak 2 is shifted from 47.6861 ms at the beginning to 204.9075 ms at the end of the test. The signal intensity of peak 1 of the

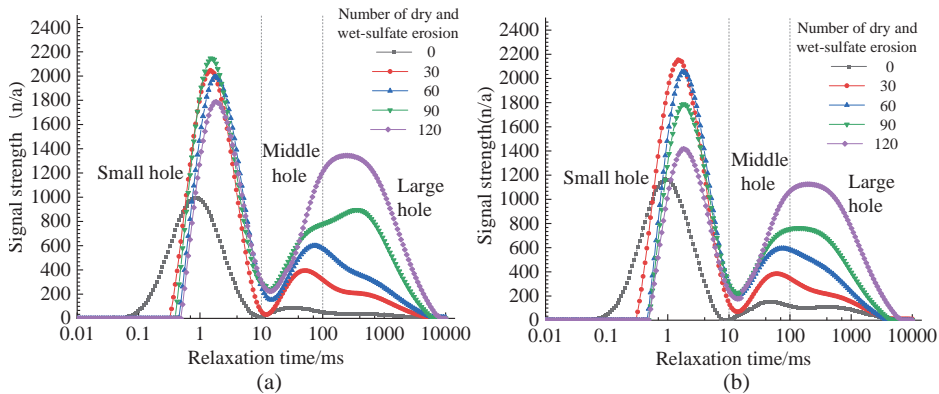


Fig. 4. Changing law of specimen pore space under the action of dry and wet sulfate erosion: a) Change of the  $T_2$  profile curve of the Q1 group, b) Change in the  $T_2$  profile curve of the Q3 group

Q3 group decreased as the number of tests increased after 30 cycles of wet and dry sulfate attack, and peak 3 increased with the increase of the number of tests; the peak 1 of the Q1 group was consistent with the Q3 group except for the increase of the signal intensity at 60–90 cycles of wet and dry-sulfate attack, and the change of peak 2 was consistent with the Q3 group. It indicates that during the dry-wet-sulfate erosion process, the small pores in the specimens of the Q1 group are continuously developing into medium-large pores while new small pores are being generated; while the change of pores in the specimens of the Q3 group is mainly based on the development of small pores into medium-large pores. It indicates that in the late stage of the dry-wet-sulfate erosion test, due to the accumulation of damage effect inside the specimens, the specimens started to show significant cracking inside the specimens. Comparing the change of pore space and the change of mass loss in the dynamic elastic moduli of the specimens in the Q1 and Q3 groups, it can be seen that polypropylene fiber can reduce the deterioration rate and damage degree of the specimens.

### 3.4. SEM electron microscopy microstructure analysis

To observe the microstructural changes inside the exemplars under the above conditions, four groups of specimens Q1, Q2, Q3, and Q4 were scanned sample by field emission electron microscopy at the end of the test, and the results of the field emission electron microscopy scans of the specimens are shown in Fig. 5.

From Fig. 5, it can be seen that in the presence of dry and wet salt attack, the surface of the microstructure of the specimen is rougher, the surface of the cement paste is severely damaged and a large number of holes exist, and a large amount of new material exists around the destroyed cement paste, and for the specimen with sulfate erosion, the free  $\text{SO}_2^-$  enters the interior of the specimen to generate a large amount of coral-like and rod-like new material by chemical reaction, which, together with the action of the dry and wet factors in The superposition of wet and dry factors finally causes the internal compactness

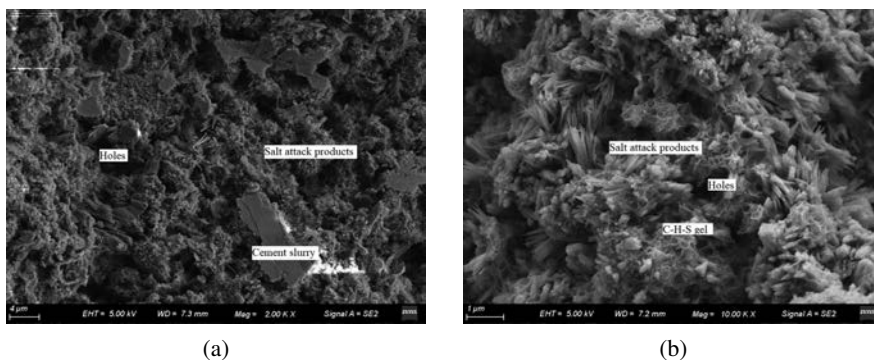


Fig. 5. SEM microstructure of the specimen. Q1 group microstructure: a)  $\times 2000$ , b)  $\times 10000$

of the specimen to decrease and cracks to develop continuously, which eventually leads to the decrease of the macroscopic deterioration index of mass loss and the dynamic elastic moduli of the specimen.

### 3.5. XRD physical phase analysis

Using SEM electron microscope scanning analysis, the internal microstructure of the specimens after the dry-wet-sulfate erosion test could be visualized. To further determine the composition of the nascent material mentioned above, the XRD technique was used to analyze the physical phase of the above specimens. The XRD diffraction results were imported into the Jade 6.5 software for phase retrieval and comparison, and the final determination of the material composition is shown in Fig. 6.

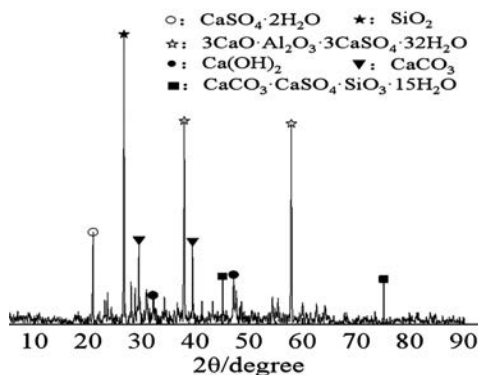


Fig. 6. XRD diffraction composition analysis

From the Fig. 6, it can be seen that the diffraction peaks of  $\text{SiO}_2$  (quartz) are the most obvious in the diffraction pattern, and these  $\text{SiO}_2$  mainly originate from the fine

aggregate, which is enriched inside the specimen because of its inactive nature and difficult to react chemically with other substances inside the specimen; from the newborn substances inside the specimen, it can be seen that the diffraction peaks related to sulfate within the specimen up obvious, especially  $3\text{CaO}\cdot\text{Al}_2\text{O}_3\cdot 3\text{CaSO}_4\cdot 32\text{H}_2\text{O}$  (Aft),  $\text{CaSO}_4\cdot 2\text{H}_2\text{O}$  and  $\text{CaCO}_3\cdot \text{CaSO}_4\cdot \text{CaSiO}_3\cdot 15\text{H}_2\text{O}$ . These substances are the same as those in the building debris obtained from the field research, indicating that the test protocol is well designed and accurately simulates the process of sulfate attack on concrete in South China.

## 4. Concrete life prediction based on damage evolution equation

### 4.1. Selection of damage variables

The so-called damage mechanics is the law of the development of damage to objects in various environments with changing deformation or time, and eventually damage [10]. Using damage mechanics theory first needs to define the damage variables, so-called damage variables, that can explain the development of material damage and have a role in the internal impact on the material. This paper selects the dynamic elastic modulo as the damage variable.

### 4.2. Establishing the damage evolution equation

By damage mechanics theory, the damage variable expression is

$$(4.1) \quad D = 1 - E_n/E_0$$

where:  $D$  is the damage variable, and  $E_0$  and  $E_n$  are the elasticity dynamic modulo before and after damage. A concrete durability experiment was conducted. In general, the relative dynamic modulus of elasticity  $E_r$  of a material is used as a measure of its durability.

$$(4.2) \quad E_r = E_n/E_0$$

Yu [11] pointed out that the relative dynamic elasticity modulo can be used to characterize the deterioration process of concrete, and the constancy of the damage failure process of concrete can be scheduled studied by measuring the change of the relative dynamic elastic modulo of concrete, therefore, the relative dynamic elasticity modulo can be used to indicate the damage evolution equation under the action of corrosion factors as follows.

$$(4.3) \quad E_{r1} = 1 + aN \quad (N < N_{12})$$

$$(4.4) \quad E_{r2} = 1 + \frac{(b-a)^2}{2c} + bN + \frac{1}{2}cN^2 \quad (N > N_{12}, \quad a < b)$$

where:  $N_{12}$  is the damage variable speed point,  $a$  is the damage initial velocity,  $b$  is the secondary damage initial velocity,  $c$  is the damage acceleration, and  $N$  is the number of dry

and wet-sulfate erosion cycles. The failure process of concrete can be measured in practical engineering by measuring the relative dynamic elastic modulus.

According to the equations constructed by P.Z. Xiao [10], the fitted constant parameters are shown in Table 4 when the polypropylene fibers are blended at 0, 0.6, 0.9, and 1.2 kg/m<sup>3</sup>, respectively.

According to the parabolic damage model, constant parameters  $a$ ,  $b$ ,  $c$  and are calculated and brought into the equation, the relationship between polypropylene fiber admixture, dry and wet-sulfate erosion cycles, and relative dynamic elastic modulo can be obtained as follows.  $R^2$  is used to measure the fit of the model to the original data, the closer  $R^2$  is to 1, the better the fit is.

$$(4.5) \quad E_r = \exp [4.666 - 0.0013N \exp (-211.48\delta_d)] \quad R^2 = 0.954$$

where:  $N$  – number of dry-wet-sulfate erosion cycles,  $\delta_d$  – polypropylene dosing,  $E_r$  – Relative dynamic modulo of elasticity.

Table 4. Damage parameters

Specimen name	Polypropylene fiber dosing (kg/m <sup>3</sup> )	$a$	$b$	$c$	$R^2$
1	0	106.62	-1.28e-1	-3.16e-4	0.981
2	0.6	105.28	-8.99e-2	-3.90e-4	0.974
3	0.9	105.15	-7.97e-2	-3.44e-5	0.983
4	1.2	105.72	-8.48e-2	-3.41e-4	0.994

### 4.3. Concrete life prediction

The use of coupled freeze-thaw cycle damage evolution equation, linking indoor tests with the outdoor environment, to forecast the operating life of concrete, is of great theoretical and practical significance to extend the operating life of the concrete and improve the level of durability research.

#### 4.3.1. Lifetime prediction methods

1. Determine the main forms of erosion suffered by the project based on the local hydrology, climate, type of structures, etc. of the project.
2. Determine the initial velocity of damage and acceleration of damage according to the test conditions and test data, and establish the damage evolution equation for different polypropylene doping amounts.
3. Calculation of the life of concrete under fast experimental conditions when  $E_r$  equals 60%, based on the damage evolution equation.
4. Calculate the expected operating life of the concrete structure under actual service conditions based on the relationship between the indoor test and the actual outdoor service environment.

### 4.3.2. Lifetime prediction

Since sulfate erosion damage dominates under the coupled action of dry and wet sulfate erosion, the operating life of concrete can be computed according to the following correspondence.

$$(4.6) \quad t = kN/M$$

where:  $t$  – operating life of the structure,  $k$ – sulfate erosion test coefficient,  $N$  – number of indoor sulfate erosion,  $M$  – the number of sulfate attack cycles a concrete structure may undergo in a year in the actual environment.

The average annual number of sulfate erosion cycles in South China is 60. According to the current rapid freeze-thaw test method, the indoor and outdoor comparison relationship between 1:10–1:15, because the test in this paper for the early age of concrete, in the corrosion solution sulfate erosion and temperature difference, compared to the more severe environment, so the sulfate erosion test coefficient to take 1:20.

According to the damage evolution equation established above, i.e., Eqs. (4.1)–(4.6). The ultimate number of freeze-thaw cycles and the life of concrete with different mix ratios under the mathematical model of single-segment damage is calculated and shown in Table 5.

Table 5. Number of cycles and lifetime of extreme sulfate erosion

Specimen number	Q1	Q2	Q3	Q4
Number of times (times)	168	216	258	285
Lifespan (years)	56	72	86	95

As can be seen from the above table, the operating life of early-age concrete gradually increases with the increase of polypropylene dosing: 56 years for 0 polypropylene dosing, 72 years for 0.6 kg/m<sup>3</sup>, 86 years for 0.9 kg/m<sup>3</sup>, and 95 years for 1.2 kg/m<sup>3</sup>, the operating life of early-age concrete is 95 years at 1.2 kg/m<sup>3</sup>.

## 5. Conclusions

1. In the sulfate erosion test, with the increase of age, the fine cracks on the initial surface gradually deepen and penetrate, the skin gradually becomes loose, the angles gradually appear to fall off, and the phenomenon of aggregate loss appears; the law of change of the mass loss rate of concrete decreases first and then increases; the law of change of corrosion resistance coefficient and relative dynamic elastic modulus is opposite to it.
2. When the concrete is subjected to the coupling effect of dry and wet cycles and sulfate erosion, its surface morphological deterioration is much greater than that of concrete under a single dry and wet cycle. At the beginning of the test, the

surface of concrete specimens gradually cracked and spalled, and at the later stage, fine aggregate spalling and coarse aggregate exposure occurred, and the specific morphological changes can be divided into four stages, and the time nodes of each stage of concrete with different ratios also differed.

3. Under the test regime set up in this paper, the mass, compressive strength, and dynamic elastic modulo of early-age concrete all increased to different degrees in the early stage of the test, and with the coupling effect, the erosion products were continuously generated, the internal damage gradually intensified, and the macroscopic indicators began to decline and accelerate.
4. Under the action of sulfate erosion, based on the principle of damage mechanics and parabolic damage model, the damage degree equation of concrete with polypropylene influence coefficient is proposed with compressive strength as the evaluation index; under the coupling action, the damage failure process is reacted with relative dynamic elastic modulo, and the relationship between different polypropylene fiber admixtures and the number of dry and wet-sulfate erosion cycles is established respectively, which can better reflect The relationship between different polypropylene fiber admixtures and the number of dry and wet-sulfate erosion cycles was established, which can better reflect the deterioration and failure law of concrete and predict the operating life of the concrete.

## References

- [1] K. Liu, S. Wang, X. Quan, et al., "Effect of iron ore tailings industrial by-product as eco-friendly aggregate on mechanical properties, pore structure, and sulfate attack and dry-wet cycles resistance of concrete", *Case Studies in Construction Materials*, vol. 17, 2022, doi: [10.1016/J.CSCM.2022.E01472](https://doi.org/10.1016/J.CSCM.2022.E01472).
- [2] A.H. Shalan and M.M. El-Gohary, "Long-Term Sulfate Resistance of Blended Cement Concrete with Waste Glass Powder", *Practice Periodical on Structural Design and Construction*, vol. 27, no. 4, 2022, doi: [10.1061/\(ASCE\)SC.1943-5576.0000731](https://doi.org/10.1061/(ASCE)SC.1943-5576.0000731).
- [3] W.Z. Taffese and L. Espinosa-Leal, "Prediction of the chloride resistance level of concrete using machine learning for durability and operating life assessment of building structures", *Journal of Building Engineering*, vol. 60, 2022, doi: [10.1016/J.JOBE.2022.105146](https://doi.org/10.1016/J.JOBE.2022.105146).
- [4] H.X. Chen and X.Q. Song, "Experimental study on the strength dispersion of recycled aggregates concrete", *Journal of Xi'an University of Science and Technology*, vol. 41, no. 2, pp. 290–297, 2021, doi: [10.13800/j.cnki.xakjdx.2021.0213](https://doi.org/10.13800/j.cnki.xakjdx.2021.0213).
- [5] M.C. Chen, Q.Q. Wen, R. Luo, et al., "Investigation on Prediction Models of Damage Evolution and Fatigue Lifetime for Reinforced Concrete Beams of Metros", *Journal of the China Railway Society*, vol. 43, no. 1, pp. 160–168, 2021, doi: [10.3969/j.issn.1001-8360.2021.01.021](https://doi.org/10.3969/j.issn.1001-8360.2021.01.021).
- [6] E. Zgheib and W. Raphael, "Study of the admixtures effect on concrete creep using Bayesian Linear Regression", *Archives of Civil Engineering*, vol. 65, no 3, pp. 127–140, 2019, doi: [10.2478/ace-2019-0039](https://doi.org/10.2478/ace-2019-0039).
- [7] B. Vakhshouri and S. Nejadi, "Prediction of Compressive Strength in Light-Wight Self- Compacting Concrete by ANFIS Analytical Model", *Archives of Civil Engineering*, vol. 61, no. 2, pp. 53–72, 2015, doi: [10.1515/ace-2015-0014](https://doi.org/10.1515/ace-2015-0014).
- [8] G. Lei, W. Jian, S.Z. Zhong, et al., "Degradation of basalt fiber concrete under the action of sulfate and dry wet cycle", *Chinese Journal of Civil Engineering*, vol. 54, no. 11, pp. 37–46, 2021, doi: [10.15951/j.tmgcxb.2021.11.001](https://doi.org/10.15951/j.tmgcxb.2021.11.001).
- [9] N. Kumar and M. Barbato, "Effects of sugarcane bagasse fibers on the properties of compressed and stabilized earth blocks", *Construction and Building Materials*, vol. 315, 2022, doi: [10.1016/j.conbuildmat.2021.125552](https://doi.org/10.1016/j.conbuildmat.2021.125552).

- 
- [10] P.Z. Xiao, R.L. Zhang, R.P. Hu, et al., “Study on the Sulfate Resistance of Concrete and the Influencing Factors of Ion Diffusion”, *Materials China*, vol. 40, no. 5, pp. 359–365, 2021, doi: [10.7502/j.issn.1674-3962.201911031](https://doi.org/10.7502/j.issn.1674-3962.201911031).
- [11] H. Yu, X. Ma, and K. Yan, “An equation for determining freeze-thaw fatigue damage in concrete and a model for predicting the service life”, *Construction and Building Materials*, vol. 137, pp. 104–116, 2017, doi: [10.1016/j.conbuildmat.2017.01.042](https://doi.org/10.1016/j.conbuildmat.2017.01.042).

Received: 2023-03-06, 2023-09-05